

This is a repository copy of *Fine structure in the alpha decay of  $^{218}\text{At}$* .

White Rose Research Online URL for this paper:  
<https://eprints.whiterose.ac.uk/147459/>

Version: Published Version

---

**Article:**

Cubiss, J. G. [orcid.org/0000-0002-5076-8654](https://orcid.org/0000-0002-5076-8654), Andreyev, A. N. [orcid.org/0000-0003-2828-0262](https://orcid.org/0000-0003-2828-0262), Barzakh, A. E. et al. (25 more authors) (2019) Fine structure in the alpha decay of  $^{218}\text{At}$ . *Physical Review C - Nuclear Physics*. 064317. ISSN 2469-9993

<https://doi.org/10.1103/PhysRevC.99.064317>

---

**Reuse**

This article is distributed under the terms of the Creative Commons Attribution (CC BY) licence. This licence allows you to distribute, remix, tweak, and build upon the work, even commercially, as long as you credit the authors for the original work. More information and the full terms of the licence here:  
<https://creativecommons.org/licenses/>

**Takedown**

If you consider content in White Rose Research Online to be in breach of UK law, please notify us by emailing [eprints@whiterose.ac.uk](mailto:eprints@whiterose.ac.uk) including the URL of the record and the reason for the withdrawal request.

**Fine structure in the  $\alpha$  decay of  $^{218}\text{At}$** 

J. G. Cubiss,<sup>1,2,\*</sup> A. N. Andreyev,<sup>1,2,3</sup> A. E. Barzakh,<sup>4</sup> B. Andel,<sup>5</sup> S. Antalic,<sup>5</sup> T. E. Coccolios,<sup>6,2</sup> T. Day Goodacre,<sup>7,8,†</sup> D. V. Fedorov,<sup>4</sup> V. N. Fedosseev,<sup>7</sup> R. Ferrer,<sup>6</sup> D. A. Fink,<sup>9,10</sup> L. P. Gaffney,<sup>6</sup> L. Ghys,<sup>6,11</sup> M. Huyse,<sup>6</sup> Z. Kalaninová,<sup>5,12</sup> U. Köster,<sup>13</sup> B. A. Marsh,<sup>7</sup> P. L. Molkanov,<sup>4</sup> R. E. Rossel,<sup>7,14</sup> S. Rothe,<sup>7,14</sup> M. D. Seliverstov,<sup>1,4</sup> S. Sels,<sup>6</sup> A. M. Sjödin,<sup>9</sup> M. Stryjczyk,<sup>6</sup> V. L. Truesdale,<sup>1</sup> C. Van Beveren,<sup>6</sup> P. Van Duppen,<sup>6</sup> and G. L. Wilson<sup>1</sup>

<sup>1</sup>*Department of Physics, University of York, York, YO10 5DD, United Kingdom*

<sup>2</sup>*ISOLDE, CERN, CH-1211 Geneva 23, Switzerland*

<sup>3</sup>*Advanced Science Research Center (ASRC), Japan Atomic Energy Agency (JAEA), Tokai-mura, Ibaraki 319-1195, Japan*

<sup>4</sup>*Petersburg Nuclear Physics Institute, NRC Kurchatov Institute, 188300 Gatchina, Russia*

<sup>5</sup>*Department of Nuclear Physics and Biophysics, Comenius University in Bratislava, 84248 Bratislava, Slovakia*

<sup>6</sup>*KU Leuven, Instituut voor Kern- en Stralingsfysica, B-3001 Leuven, Belgium*

<sup>7</sup>*CERN, CH-1211 Geneva 23, Switzerland*

<sup>8</sup>*School of Physics and Astronomy, The University of Manchester, Manchester M13 9PL, United Kingdom*

<sup>9</sup>*Engineering Department, CERN, CH-1211 Geneva 23, Switzerland*

<sup>10</sup>*Ruprecht-Karls Universität, D-69117 Heidelberg, Germany*

<sup>11</sup>*Belgian Nuclear Research Centre SCK CEN, Boeretang 200, B-2400 Mol, Belgium*

<sup>12</sup>*Laboratory of Nuclear Problems, JINR, 141980 Dubna, Russia*

<sup>13</sup>*Institut Laue Langevin, 6 rue Jules Horowitz, F-38042 Grenoble Cedex 9, France*

<sup>14</sup>*Institut für Physik, Johannes Gutenberg-Universität, D-55099 Mainz, Germany*



(Received 18 March 2019; published 14 June 2019)

An  $\alpha$ -decay study of  $^{218}\text{At}$  was performed at the CERN-ISOLDE facility. Laser-ionized beams of  $^{218}\text{At}$  were mass separated and implanted into an  $\alpha$ - $\gamma$  detection setup. Coincidence  $\alpha$ - $\gamma$  data were collected for the first time and a more precise half-life value of  $T_{1/2} = 1.27(6)$  s was measured. A new  $\alpha$ -decay scheme was deduced based on the extracted reduced  $\alpha$ -decay widths for fine-structure decays. The results from this work lead to a preferred spin and parity assignment of  $J^\pi = (3^-)$ ; however,  $J^\pi = (2)^-$  cannot be fully excluded.

DOI: [10.1103/PhysRevC.99.064317](https://doi.org/10.1103/PhysRevC.99.064317)

**I. INTRODUCTION**

The isotopes found northeast of doubly magic  $^{208}\text{Pb}$  in the nuclear chart with  $130 \leq N \leq 140$  and  $85 \leq Z \leq 93$  are expected to possess octupole correlations [1], which are caused by the proximity of the Fermi surface to orbitals with  $\Delta j = \Delta \ell = 3$ . In particular, for the aforementioned region, the  $2f_{7/2}$  and  $1i_{13/2}$  proton, and the  $2g_{9/2}$  and  $1j_{15/2}$  neutron orbitals play an important role in the governance of the underlying structures [2].

The influence of octupole correlations on the ground states of  $^{217-219}\text{At}$  ( $Z = 85$ ,  $N = 132-134$ ) was studied at the CERN-ISOLDE facility via in-source laser spectroscopy measurements of the hyperfine structures (hfs) and isotope shifts (IS), the results of which are presented in a complementary

paper [3]. Based on such data, the nuclear electromagnetic moments and changes in mean-squared charge radii were deduced. However, knowledge of the nuclear spin is required in order to extract this information from the measured hfs and IS. Little is known about the structure of  $^{218}\text{At}$ , for which the current  $J^\pi = (1^-)$  spin and parity assignment (quoted by NNDC [4]) is based on systematics alone.

The current work presents the results from an  $\alpha$ -decay study of  $^{218}\text{At}$ , which could provide further information on the spin of its ground state. Both the decay data of the present work and the hfs and IS measurements [3] were taken during the experiment described in detail in Ref. [5].

Alpha decay is a powerful tool for investigating nuclear states at low excitation energies, due to its strong sensitivity to the  $Q_\alpha$  value. Furthermore, alongside the strong dependence of its partial half-life on changes in spin between the connected states, it has a high sensitivity to differences in structure between the parent and daughter nuclei which can be quantified by using reduced  $\alpha$ -decay widths ( $\delta_\alpha^2$ ) or hindrance factors ( $HF_\alpha$ ) [6].

The first information on the  $\alpha$ -decay properties of  $^{218}\text{At}$  came from studies of the  $\alpha$ -decay chain of the long-lived isotope  $^{226}\text{Ra}$  [ $T_{1/2} = 1600(7)$  y [4]], conducted in the 1940s and 1950s by Walen and Bastin [7,8] who used a magnetic

\*james.cubiss@york.ac.uk

†Present address: TRIUMF, 4004 Wesbrook Mall, Vancouver BC V6T 2A3, Canada.

Published by the American Physical Society under the terms of the [Creative Commons Attribution 4.0 International](https://creativecommons.org/licenses/by/4.0/) license. Further distribution of this work must maintain attribution to the author(s) and the published article's title, journal citation, and DOI.

spectrometer to measure the energies of  $\alpha$  particles. Two  $\alpha$ -decay lines at  $E_\alpha = 6653(5)$  keV ( $I_{\text{rel}} = 6\%$ ) and  $6697(3)$  keV ( $I_{\text{rel}} = 94\%$ ) were identified (see Fig. 1 of Ref. [8]), and a half-life of  $1.3(1)$  s was extracted for the ground state of  $^{218}\text{At}$ . A second study by the same group using the same technique confirmed the decays with  $E_\alpha = 6654$  keV ( $I_{\text{rel}} = 6.4\%$ ),  $6694$  keV ( $I_{\text{rel}} = 90\%$ ), and claimed a third,  $E_\alpha = 6757$  keV ( $I_{\text{rel}} = 3.6\%$ ) decay, as cited in the textbook [9]. The energies of the three  $\alpha$  decays were later evaluated to be  $E_\alpha = 6653(5)$ ,  $6693(3)$ , and  $6756(5)$  keV [10]. However, it is important to stress that the data for the third  $\alpha$  decay referenced in Ref. [9] were taken from private communications. To our knowledge, neither the original experimental data nor spectra were published. We note that, based on the reported intensity of the highest-energy line at  $E_\alpha = 6756$  keV in Ref. [9], this decay should have been seen in the first study [8]. However, no such line is present in the spectrum in Fig. 1 of Ref. [8]. Therefore, one of the aims of the present study was to verify the presence of the highest-energy  $\alpha$  line of  $^{218}\text{At}$ , referenced in Ref. [9].

Published information on the daughter nucleus  $^{214}\text{Bi}$  comes from a series of  $\beta$ -decay studies of  $^{214}\text{Pb} \rightarrow ^{214}\text{Bi}$  [11–16] and  $^{214}\text{Bi} \rightarrow ^{214}\text{Po}$  [17]. Together, these studies firmly established  $J^\pi(^{214}\text{Bi}^g) = 1^-$ , with a most probable  $\pi 1h_{9/2} \otimes \nu 2g_{9/2}$  configuration. Furthermore and of importance to the present work, two low-lying, negative-parity states at excitation energies of 53 and 63 keV were deduced. These states were suggested to be members of the same  $\pi 1h_{9/2} \otimes \nu 2g_{9/2}$  multiplet, with most probable spins and parities of  $J^\pi = (2)^-$  and  $(3)^-$ , respectively [15,16].

The current work represents the first study in which direct measurements of  $\gamma$ -ray transitions following the  $\alpha$  decay of  $^{218}\text{At}$  have been made.

## II. EXPERIMENT

The  $^{218}\text{At}$  nuclei were produced at the ISOLDE facility [18,19] in spallation reactions induced by a 1.4 GeV proton beam, impinging upon a 50-g  $\text{cm}^{-2}$ -thick uranium carbide target. The proton beam was delivered by the CERN PS Booster, with an average current of  $\approx 1.5$   $\mu\text{A}$ , in a repeated sequence known as a supercycle. Each supercycle typically consisted of 35–40, 2.4- $\mu\text{s}$ -long pulses, with a minimum interval of 1.2 s between consecutive pulses.

After proton impact, the reaction products diffused through the target matrix and effused towards a hot cavity ion source, kept at a temperature of  $\approx 2300$  K. Inside the cavity, the  $^{218}\text{At}$  atoms were selectively ionized by using a three-step resonance laser ionization scheme (see Fig. 1 of Ref. [5]), delivered by the ISOLDE Resonance Ionization Laser Ion Source (RILIS) [20,21]. The ions were then extracted from the cavity by using a 30 kV electrostatic potential and separated according to their mass-to-charge ratio by the ISOLDE general purpose separator magnet.

The mass-separated ion beam was then delivered to the Windmill decay station [22,23] for decay measurements. The ion beam entered the Windmill system through the center hole of an annular silicon detector (Si1) and was implanted into one of ten, 20- $\mu\text{g}$   $\text{cm}^{-2}$ -thick carbon foils mounted

on a rotatable wheel. A second silicon detector (Si2) was positioned a few millimeters behind the foil being irradiated. Together, Si1 + Si2 were used to measure the short-lived  $\alpha$  activity at the implantation site. After a fixed number of supercycles, the wheel of the Windmill was rotated (rotation time  $\approx 0.8$  s), moving the irradiated foil to a decay site, between a pair of closely spaced silicon detectors (Si3 and Si4), which were used to measure long-lived daughter decays. The full widths at half maximum of the recorded  $\alpha$ -decay peaks within the energy region of interest ( $E_\alpha = 6000$ – $8000$  keV), were 30–40 keV.

In addition to the silicon detectors, a single crystal, low-energy germanium (LEGe) detector was placed outside of the Windmill chamber directly behind Si2, for  $\gamma$ - and x-ray detection. Energy and efficiency calibrations were made by using standard sources of  $^{60}\text{Co}$ ,  $^{133}\text{Ba}$ ,  $^{137}\text{Cs}$ , and  $^{152}\text{Eu}$ .

## III. RESULTS

### A. Singles $\alpha$ -decay spectrum of $^{218}\text{At}$

Figure 1(a) shows the sum singles  $\alpha$ -decay spectrum for Si1 + Si2 collected at  $A = 218$ , in which the  $^{218}\text{At}$   $\alpha$  decays can be seen in the  $6600 < E_\alpha < 6800$  keV region, along with decays belonging to surface-ionized isobaric  $^{218}\text{Fr}$  at  $E_\alpha > 7000$  keV. The nonobservation of any  $E_\alpha = 7129.2(12)$  keV decays of  $^{218}\text{Rn}$  [10] proves that  $^{218}\text{At}$  has a negligible  $\beta$ -decay probability, which is in agreement with the  $\alpha$ -decay branching ratio of  $b_\alpha(^{218}\text{At}) = 99.9\%$  suggested in Ref. [7]. Energy calibrations for the silicon detectors were made by using the well-known  $\alpha$ -decay energies of  $^{218}\text{Fr}$  [ $E_\alpha = 7238(5)$ ,  $7951(5)$ ,  $8782(5)$  keV], along with  $\alpha$  decays of  $^{199}\text{At}$  [ $E_\alpha = 6643(3)$  keV] measured in a neighboring run, at  $A = 199$ .

A complex structure with three components (the component labeled “6760” will be discussed in detail in Sec. IV A) can be seen in the inset of Fig. 1(a), which zooms in on the  $\alpha$  decay of  $^{218}\text{At}$ . This spectrum was fit with Crystal Ball functions, using the ROOT Minuit minimizer, a binned-likelihood method and an assumption of three  $\alpha$ -decay peaks. The fit yielded  $\alpha$ -decay energies of  $E_\alpha = 6655(7)$ ,  $6694(5)$ , and  $6741(7)$  keV. The former two are in good agreement with the previous studies [8,9]; however, the  $E_\alpha = 6741$  keV is 15 keV lower than the 6756 keV  $\alpha$  line referenced in Ref. [9]. It will be shown in Sec IV A that this is an artificial peak due to  $\alpha +$  conversion electron ( $\alpha + e^-$ ) summing within the silicon detectors.

### B. $\alpha$ - $\gamma$ coincidences

Prompt  $\alpha$ - $\gamma$  coincidence data between the Si1 and Si2 detectors and the LEGe, with the timing condition  $\Delta T(\alpha\text{-}\gamma) \leq 300$  ns, are shown in Fig. 1(b). The projection on the  $E_\gamma$  axis for the  $\alpha$  decays of  $^{218}\text{At}$  is shown in Fig. 1(c). An  $\alpha$ - $\gamma$  coincidence group attributed in this work to the fine-structure decay of  $^{218}\text{At}$  is seen at  $6694\text{-}53.3(3)$  keV, along with a number of other  $\alpha$ - $\gamma$  coincidence groups belonging to the decay of  $^{218}\text{Fr}$ .<sup>1</sup> The observation of the  $6694\text{-}53.3$  keV group

<sup>1</sup>The latter are not within the scope of the current study and so will not be discussed further in this work.

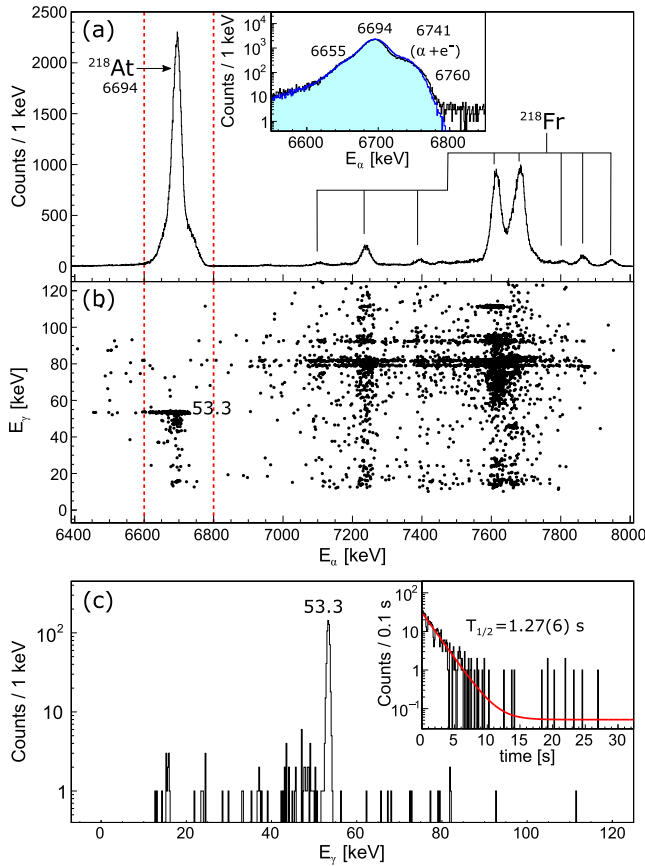


FIG. 1. (a) Sum of singles  $\alpha$ -decay spectra recorded in Si1 + Si2 detectors, for  $A = 218$ . The inset of panel (a) shows the singles  $\alpha$ -decay spectrum (black histogram), zoomed in on the energy region of  $^{218}\text{At}$  and overlapped with results from GEANT4 simulations (blue histogram, see Sec. IV A for more details). (b)  $\alpha$ - $\gamma$  coincidences for  $\alpha$ -decay data shown in panel (a), measured within a  $\Delta T(\alpha\text{-}\gamma) \leq 300$  ns time interval. (c) Projection on the  $E_\gamma$  axis of panel (b), for the gating condition  $6600 < E_\alpha < 6800$  keV (indicated by vertical, red dashed lines). The inset of panel (c) shows the decay curve for  $^{218}\text{At}$  extracted from the Si3 + Si4 detectors, fit with an exponential plus a constant background.

proves that the decay path of  $^{218}\text{At}$  passes through the known 53 keV level in  $^{214}\text{Bi}$ , as shown in the decay scheme in Fig. 2. The reason behind the direct feeding of the 6694 keV  $\alpha$  decay to the 63 keV level in this scheme, rather than to the 53 keV state, will be explained in Sec. IV B.

We note that no 63 keV  $\gamma$ -ray transition is seen in coincidence with the  $\alpha$  decays of  $^{218}\text{At}$  in Figs. 1(b) and 1(c). The 63 keV level was originally inferred from high-statistics  $\gamma$ - $\gamma$  coincidence data and assigned a most probable  $J^\pi = (3^-)$  [15,16]. The nonobservation of this  $\gamma$  decay was explained in Ref. [16] (see Sec. III.D.4 therein) due to a strong preference for a  $63 \rightarrow 53 \rightarrow 0$  keV cascade of  $M1$  transitions relative to a direct 63 keV  $E2$  transition, for which relative probabilities of  $>91\%$  and  $<9\%$  were evaluated, respectively. In this scenario, an  $\approx 10$  keV transition between the 63 and 53 keV levels would not be observed experimentally due to its low energy

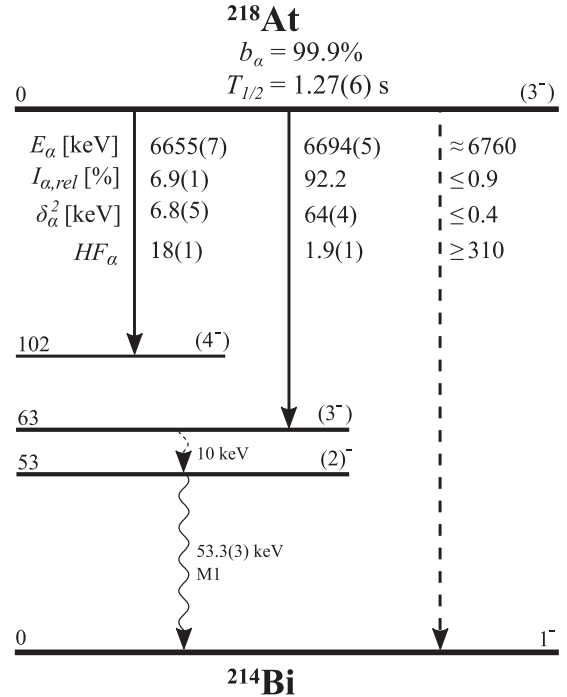


FIG. 2. The preferred decay scheme for  $^{218}\text{At}$  deduced from the present work, with  $b_\alpha(^{218}\text{At}) = 99.9\%$  taken from Ref. [7]. The  $\alpha$  decays and  $\gamma$ -ray transition observed in the present data are represented by the solid straight and curly arrows, respectively, and the dashed lines represent the possible, yet currently unobserved transitions. The hindrance factors were calculated relative to the unhindered,  $\delta_\alpha^2 = 124(1)$  keV,  $9/2^- \rightarrow 9/2^-$   $\alpha$  decay of the neighboring odd-mass isotope,  $^{217}\text{At}$  [4].

and high conversion coefficient ( $\alpha_{c,tot} > 400$  [24]). Thus, we do not expect to see the 63 keV  $\gamma$  line in our data.

A total conversion coefficient of  $\alpha_{tot,expt}(53.3 \text{ keV}) = 8.6(4)$  was deduced by comparing the number of  $\alpha$ - $\gamma$  coincidences,  $N_{\alpha\gamma}$ , shown in Figs. 1(b) and 1(c), corrected for  $\gamma$ -decay detection efficiency  $\epsilon_\gamma$ , with the number of singles  $\alpha$ -decay events,  $N_\alpha$ , from Fig. 1(a) such that

$$\alpha_{tot,expt} = \frac{N_\alpha \epsilon_\gamma}{N_{\alpha\gamma}} - 1. \quad (1)$$

This value is closest to the calculated value  $\alpha_{tot,calc}(M1) = 11.99(17)$  and much lower than  $\alpha_{tot,calc}(E2) = 127.5(18)$  [24], confirming the near-pure  $M1$  assignment of previous studies [11–16].

### C. Determination of the $^{218}\text{At}$ half-life

The half-life of  $^{218}\text{At}$  was determined from the pure decay data recorded in the Si3 + Si4 detectors (i.e., no new activity was implanted into the foil positioned between Si3 + Si4, during the measurement of the decay curve). The extracted decay curve, shown in the inset of Fig. 1(c), was fit with an exponential function plus a constant background by using a binned-likelihood method, from which  $T_{1/2} = 1.27(6)$  s was deduced. This result agrees with but has a higher precision



than the tabulated values of  $T_{1/2} = 1.5(3)$  s [25] and  $T_{1/2} = 1.3(1)$  s [8].

#### IV. DISCUSSION

##### A. $\alpha$ - $e^-$ summing

The strong conversion of the 53.3 keV  $\gamma$  transition can produce  $\alpha + e^-$  summing, if both the energy of the 6694 keV  $\alpha$  decay and a subsequent conversion electron are registered simultaneously in the same silicon detector. To understand the magnitude of this effect, GEANT4 [26,27] simulations were performed to see how conversion electrons from the deexcitation of the 63 keV level in  $^{214}\text{Bi}$  would affect the singles spectrum shown in Fig. 1(a).

The simulations included conversion electrons and the relevant x rays for both a  $63 \rightarrow 0$  keV  $E2$   $\gamma$  transition and a  $63 \rightarrow 53 \rightarrow 0$  keV,  $M1$ - $M1$  cascade decay branches, using a branching ratio of 9% for the former taken from the upper limit given in Ref. [16]. In addition, conversion electrons due to a cascade of three  $M1$  transitions were used to simulate the deexcitation of the 102 keV level, populated by the 6655 keV  $\alpha$  line. Auger electrons were not included in the simulations because their contribution to the main  $\alpha + e^-$  sum peaks would be negligible due to their low energies. For the  $53 \rightarrow 0$  keV transition the conversion coefficient deduced in the present work was used ( $\alpha_{tot,expt} = 8.6$ ). The results of the simulations, shown by the blue histogram in the inset of Fig. 1(a), indicate that the 6741 keV peak is an artificial  $\alpha$ -decay peak due to  $\alpha + e^-$  summing and thus should not be considered when building the decay scheme, apart from adding its intensity to that of the  $E_\alpha = 6994$  keV decay.

Based on the simulations a scenario could be considered in which only two  $\alpha$  decays belong to  $^{218}\text{At}$ , with energies of  $E_\alpha = 6655$  and 6694 keV. These two decays would have intensities of  $I_\alpha(6655) = 6.9(1)\%$  and  $I_\alpha(6694) = 93.1(1)\%$ , which is in good agreement with the results of Ref. [8].

However, a closer inspection of the experimental data in the inset of Fig. 1(a) shows that a small excess of events exists at  $E_\alpha \approx 6760$  keV compared with the results of the GEANT4 simulations. This excess could be due to a third  $\alpha$ -decay. By subtracting the simulated spectrum from the experimental data a small peak remains with  $E_\alpha \approx 6760$  keV. This remaining peak may correspond to the highest-energy  $E_\alpha = 6756$  keV line cited in Ref. [9]. Based on the intensity of the remaining peak, a lower limit of  $I_\alpha \geq 92.2\%$  ( $1\sigma$ ) for the 6694 keV  $\alpha$  line and an upper limit of  $I_\alpha \leq 0.9\%$  ( $1\sigma$ ) for the possible 6760 keV decay can be extracted. The main source of uncertainty in these intensity values stems from a  $\pm 0.5$  mm uncertainty in the exact positions of Si1 and Si2 relative to the implantation foil. The  $I_\alpha(6760)$  is smaller than  $I_\alpha(6756) = 3.6\%$  referenced in Ref. [9] (see Table I for comparison). Therefore, this  $\alpha$ -decay line is included only tentatively in Fig. 2.

##### B. Proposed decay scheme for $^{218}\text{At}$

In Ref. [15], the 6694 and 6655 keV  $\alpha$  decays were assigned to feed directly to the 63 keV level and a 102 keV excited states in  $^{214}\text{Bi}$ , respectively, based on their difference

TABLE I. Comparison of the  $E_\alpha$  and  $I_\alpha$  values from the present work and previous studies [9,10], assuming three  $\alpha$  decays belonging to  $^{218}\text{At}$ .

Si1 + Si2 (present work)		Refs. [9,10]	
$E_\alpha$ [keV]	$I_\alpha$ [%]	$E_\alpha$ [keV]	$I_\alpha$ [%]
6655(7)	6.9(1)	6653(5)	6.4
6694(5)	92.2	6693(3)	90
$\approx 6760$	$\leq 0.9$	6756(5)	3.6

in  $Q_\alpha$  with the 6756 keV decay cited in Ref. [9]. The results from the present work are consistent with these assignments, with the tentative  $E_\alpha \approx 6760$  keV decay representing the ground-to-ground state  $\alpha$  decay, as shown in Fig. 2.

Before continuing further, it is informative to study the available, albeit sparse,  $HF_\alpha$  systematics for fine-structure  $\alpha$  decays between states of the  $\pi 1h_{9/2} \otimes \nu 2g_{9/2}$  multiplet in neighboring nuclei, provided in Table II. Here, it is seen that decays with  $J_i = J_f = 1^-$  are unhindered, with typical  $HF_\alpha \approx 2$ . In contrast to this, decays with  $J_i \neq J_f$  are hindered. One would expect the  $1^- \rightarrow 3^-$   $\alpha$  decays to be more hindered than  $1^- \rightarrow 2^-$  decays. This is true for  $^{216}\text{At}$  and  $^{216}\text{Fr}$ ; however,  $^{214}\text{At}$  does not follow this pattern. The latter observation is currently not understood but it could be due to states with a mixed  $\nu 2g_{9/2}$  and  $\nu 1i_{11/2}$  component of their configuration, as suggested in Ref. [28]. Therefore, while a low  $HF_\alpha$  is a good indication of  $\alpha$  decay between states of the same spin and configuration, the use of systematics for hindered decays to extract information on the spin is less reliable.

The  $\delta_\alpha^2$  values for the  $^{218}\text{At}$  fine-structure decays, shown in Fig. 2 were deduced using the Rasmussen approach [31] with an assumption of  $\Delta L = 0$ . The  $HF_\alpha$  values were calculated relative to the unhindered,  $\delta_\alpha^2 = 124(1)$  keV,  $9/2^- \rightarrow 9/2^-$   $\alpha$  decay of the neighboring odd-mass isotope,  $^{217}\text{At}$  [4]. The unhindered nature of the 6694-keV  $\alpha$  decay suggests that the ground state of  $^{218}\text{At}$  has the same structure and spin as the  $J^\pi = (3^-)$ , 63 keV level in  $^{214}\text{Bi}$  that it feeds to. On the other hand, the large hindrance of the tentative  $E_\alpha = 6760$  keV decay ( $HF_\alpha \geq 310$ ) suggests that the ground-state configurations of  $^{218}\text{At}$  and  $^{214}\text{Bi}$  are quite different.

One could tentatively propose that the 102 keV state fed by the 6655 keV decay is the  $J^\pi = (4^-)$  member of the  $\pi 1h_{9/2} \otimes \nu 2g_{9/2}$  multiplet. This proposal is consistent with the fact that no such level was identified in the previous  $^{214}\text{Pb} \rightarrow ^{214}\text{Bi}$   $\beta$ -decay studies [13–16], as this would require a third-order forbidden decay ( $J^\pi = 0^+ \rightarrow 4^-$ ) that would be slow relative to the dominant allowed and first-forbidden decay channels. The statistics collected in the present work are not sufficient to observe deexcitations from the 102 keV level.

It is also necessary to consider a possible  $E_\alpha = 6704$  keV decay to the 53 keV,  $J^\pi = (2)^-$  level in  $^{214}\text{Bi}$ . A broadening of the  $E_\alpha = 6694$  keV peak relative to other peaks in the spectrum and a shift in its centroid energy relative to the tabulated values would provide evidence for this decay branch. However, no such effect is seen in the present data, placing an upper limit on the intensity of  $I_\alpha(6704) < 7\%$ .

TABLE II. Comparison of hindrance factors from Refs. [28–30] and the present work, for  $\alpha$  decays between states of varying spins, and assuming the configurations of the initial and final states have a dominant  $\pi 1h_{9/2} \otimes \nu 2g_{9/2}$  component.

Isotope	$E_\alpha$ [keV]	$I_\alpha$ [%]	$J_i^\pi \rightarrow J_f^\pi$	$HF_\alpha$	Ref.
$^{216}\text{Fr}$	8811(15)	$\approx 0.2$	$(1^-) \rightarrow (3^-)$	280	[30]
	8861(15)	0.5(2)	$(1^-) \rightarrow (2^-)$	180	
	9004(5)	95(1)	$(1^-) \rightarrow (1^-)$	2.5	
$^{216}\text{At}$	7595	0.16(5)	$1^- \rightarrow (3^-)$	300	[29]
	7691	1.4(2)	$1^- \rightarrow 2^{(-)}$	67	
	7804	97.5	$1^- \rightarrow 1^{(-)}$	2	
$^{214}\text{At}$	8469	0.6	$1^- \rightarrow 3^-$	35	[28]
	8500	0.2	$1^- \rightarrow 2^-$	160	
	8812	99	$1^- \rightarrow 1^-$	1.5	
$^{218}\text{At}$	6655(7)	6.9(1)	$(3^-) \rightarrow (4^-)$	18(1)	Present work
	6694(5)	92.2	$(3^-) \rightarrow (3^-)$	1.9(1)	
	$\approx 6760$	$\leq 0.9$	$(3^-) \rightarrow 1^-$	$\geq 310$	

Returning to the discussion on the  $E_\alpha \approx 6760$  keV decay, we remind the reader that the upper limit for the intensity deduced in the present work is much lower than that reported in Ref. [9]. Additionally, it is important to note that the 6756 keV  $\alpha$  decay was not observed in the original study [8] and that it cannot be explained by  $\alpha + e^-$  summing in Ref. [9] (as in the present work) due to the use of a magnetic spectrometer during the experiment. Together, these two points make the existence of a 6760 keV  $\alpha$  decay questionable. In the scenario where the 6760 keV  $\alpha$  decay is absent, the  $E_\alpha = 6694$  keV decay would be assigned to feed directly to the 53 keV state in  $^{214}\text{Bi}$ , leading to a  $J^\pi(^{218}\text{At}) = (2^-)$  assignment. Thus, while  $J^\pi = (3^-)$  is preferred for  $^{218}\text{At}^g$ , a  $J^\pi = (2^-)$  assignment cannot be fully excluded within the precision of the present work.

### C. Energy systematics of low-lying states in even- $A$ bismuth isotopes

Energies of the  $J^\pi = 2^-, 3^-$ , and  $4^-$  states relative to the  $J^\pi = 1^-$  ground states in  $^{210,212,214}\text{Bi}$  along with their isotones  $^{212,214,216}\text{At}$  are shown in Figs. 3(a) and 3(b), respectively. The energies of the  $J^\pi = 2^- - 4^-$  states in the bismuth isotopes are seen to compress with increasing neutron number. This pattern was reproduced by the calculations for the  $\pi 1h_{9/2} \otimes \nu 2g_{9/2}$  multiplet in  $^{210,212,214,216}\text{Bi}$ , made in Ref. [32] (see Fig. 4 therein). We note that the energy for the tentative  $J^\pi = (4^-)$  state in  $^{214}\text{Bi}$  fits well with the observed systematics.

The states in the astatine ( $Z = 85$ ) isotones also display a compression in energy. While in the present work we propose a  $J^\pi = (3^-)$  ground state in  $^{218}\text{At}$ , a  $J^\pi = 1^-, 2^-$  or  $4^-$  assignment would seem more favorable from the systematics displayed in Fig. 3(b). This discrepancy remains unexplained.

## V. CONCLUSION

The  $\alpha$ -decay study of  $^{218}\text{At}$  including the first direct measurements of prompt  $\alpha$ - $\gamma$  coincidences has been made at the CERN-ISOLDE facility. Based on the results from the

present work and those of Refs. [15,16], a ground-state spin and parity assignment of  $J^\pi = (3^-)$  is proposed for  $^{218}\text{At}$ . However, we note that a  $J^\pi = (2^-)$  assignment cannot be fully excluded.

Both the possible  $J^\pi = (3^-)$  and  $(2^-)$  assignments for the ground state of  $^{218}\text{At}$  disagree with the current  $J^\pi = 1^-$  proposed in Ref. [33], which is based on systematics alone. Therefore, both options should be probed in the analysis of the hfs of  $^{218}\text{At}$ , in the complementary paper [3].

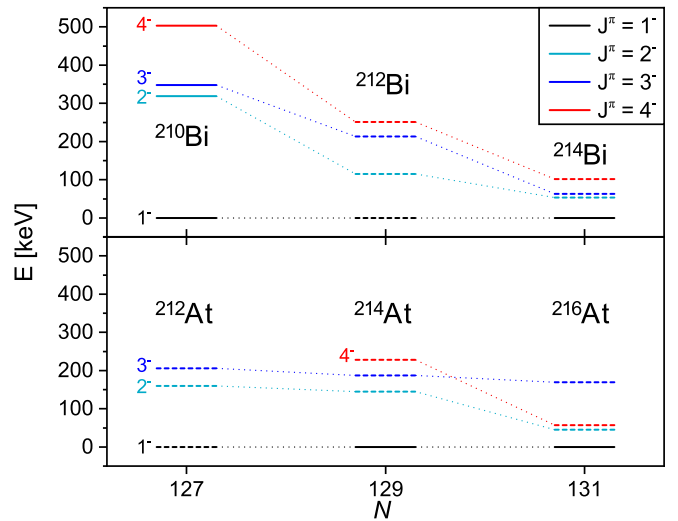


FIG. 3. Excitation energies of the low-spin states that are presumed to have a configuration with a dominant  $\pi 1h_{9/2} \otimes \nu 2g_{9/2}$  component, relative to the  $J^\pi = 1^-$  ground states of (a)  $^{210,212,214}\text{Bi}$  and (b) their respective isotones,  $^{212,214,216}\text{At}$ . States with the same spin and parity are connected by dotted lines. States with tentative spin, parity, or spin and parity assignments are indicated by a dashed line. The energy for the  $J^\pi = (4^-)$  state in  $^{214}\text{Bi}$  is taken from the tentative assignment proposed in the current work, whereas other data are taken from the Evaluated Nuclear Structure Data File [4].

## ACKNOWLEDGMENTS

We would like to acknowledge the support of the ISOLDE Collaboration and technical teams. This work was done with support from the European Union's Seventh Framework Programme for Research and Technological Development under Grant Agreements 262010 (ENSAR), 267194 (COFUND), and 289191 (LA<sup>3</sup>NET), by grants from the UK Science and

Technology Facilities Council (STFC), by FWO-Vlaanderen (Belgium), by GOA/2010/010 (BOF KU Leuven), by the Interuniversity Attraction Poles Programme initiated by the Belgian Science Policy Office (BriX network P7/12), by RFBF according to the research Project No. 19-02-00005, by the Slovak Research and Development Agency (Contract No. APVV-14-0524) and the Slovak Grant Agency VEGA (Contract No. 1/0532/17).

- 
- [1] P. A. Butler, *J. Phys. G* **43**, 073002 (2016).
- [2] P. A. Butler and W. Nazarewicz, *Rev. Mod. Phys.* **68**, 349 (1996).
- [3] A. E. Barzakh *et al.*, *Phys. Rev. C* **99**, 054317 (2019).
- [4] NNDC, Evaluated Nuclear Structure Data File (2017).
- [5] J. G. Cubiss *et al.*, *Phys. Rev. C* **97**, 054327 (2018).
- [6] P. Van Duppen and M. Huyse, *Hyperfine Interact.* **129**, 149 (2000).
- [7] R. J. Walen, *J. Phys. Radium* **10**, 95 (1949).
- [8] R. J. Walen and G. Bastin, in *Comptes Rendus du Congrès International de Physique Nucléaire*, edited by P. Gugenberger (Dunod, Paris, 1958).
- [9] R. J. Walen (private communication to Hyde) (1963); quoted by E. K. Hyde, I. Perlman, and G. T. Seaborg: *The Nuclear Properties of the Heavy Elements*, Vol. II (Prentice-Hall, Englewood Cliffs, NJ, 1964), p. 461.
- [10] A. Rytz, *At. Data Nucl. Data Tables* **47**, 205 (1991).
- [11] K. Nielsen, O. Nielsen, and M. Waggoner, *Nucl. Phys.* **2**, 476 (1956).
- [12] R. J. Walen and G. Bastin-Scoffier, *Nucl. Phys.* **16**, 246 (1960).
- [13] E. W. A. Lingeman, J. Konijn, P. Polak, and A. H. Wapstra, *Nucl. Phys. A* **133**, 630 (1969).
- [14] I. Penev, W. Andrejtscheff, C. Protochristow, and Z. Zhelev, *Zeitschrift für Physik A Atomic Nuclei* **318**, 213 (1984).
- [15] G. Mouze, O. Diallo, P. Bechlich, J. F. Comanducci, and C. Ythier, *Radiochim. Acta* **49**, 13 (1990).
- [16] Z. Berant, R. B. Schuhmann, D. E. Alburger, W. T. Chou, R. L. Gill, E. K. Warburton, and C. Wesselborg, *Phys. Rev. C* **43**, 1639 (1991).
- [17] A. H. Wapstra and N. B. Gove, *Nucl. Data, Sect. B* **1**, 7 (1966).
- [18] E. Kugler, *Hyperfine Interact.* **129**, 23 (2000).
- [19] R. Catherall *et al.*, *J. Phys. G* **44**, 094002 (2017).
- [20] V. I. Mishin *et al.*, *Nucl. Instrum. Methods Phys. Res., Sect. B* **73**, 550 (1993).
- [21] V. Fedosseev *et al.*, *J. Phys. G* **44**, 084006 (2017).
- [22] H. De Witte *et al.*, *Phys. Rev. Lett.* **98**, 112502 (2007).
- [23] A. N. Andreyev *et al.*, *Phys. Rev. Lett.* **105**, 252502 (2010).
- [24] T. Kibédi, T. W. Burrows, M. B. Trzhaskovskaya, P. M. Davidson, and C. W. Nestor, *Nucl. Instrum. Methods Phys. Res., Sect. A* **589**, 202 (2008).
- [25] D. G. Burke *et al.*, *Zeitschrift für Physik A Atomic Nuclei* **333**, 131 (1989).
- [26] S. Agostinelli *et al.*, *Nucl. Instrum. Methods Phys. Res., Sect. A* **506**, 250 (2003).
- [27] J. Allison *et al.*, *Nucl. Instrum. Methods Phys. Res., Sect. A* **835**, 186 (2016).
- [28] R. K. Sheline, P. Alexa, C. F. Liang, and P. Paris, *Phys. Rev. C* **59**, 101 (1999).
- [29] C. F. Liang, P. Paris, and R. K. Sheline, *Phys. Rev. C* **49**, 1872 (1994).
- [30] C. F. Liang, P. Paris, R. K. Sheline, P. Alexa, and A. Gizon, *Phys. Rev. C* **54**, 2304 (1996).
- [31] J. O. Rasmussen, *Phys. Rev.* **113**, 1593 (1959).
- [32] J. Kurpeta, A. Andreyev, J. Aysto, A.-H. Evensen, M. Huhta, M. Huyse, A. Jokinen, M. Karny, E. Kugler, J. Lettry, A. Nieminen, A. Plochocki, M. Ramdhane, H. L. Ravn, K. Rykaczewski, J. Szerypo, P. V. Duppen, G. Walter, and A. Wöhr, *Eur. Phys. J. A* **7**, 49 (2000).
- [33] G. Audi, O. Bersillon, J. Blachot, and A. Wapstra, *Nucl. Phys. A* **729**, 3 (2003), the 2003 NUBASE and Atomic Mass Evaluations.